Pergamon

PII: S0191-8141(96)00108-3

Journal of Structural Geology, Vol. 19, Nos 3–4, pp. 503 to 521, 1997

0191-8141/97 $17.00 + 0.00

Structural evolution of connecting splay duplexes and their implications for critical taper: an example based on geometry and kinematics of the Canyon Range culmination, Sevier Belt, central Utah

GAUTAM MITRA and AVIVA J. SUSSMAN

Department of Earth and Environmental Sciences, University of Rochester, Rochester, NY 14627, U.S.A.

(*Received* 21 *February* 1996; *accepted in revised form* 12 *November* 1996)

Abstract—Critical taper in an evolving orogenic wedge can be maintained by structural thickening in the back of the wedge. This is often achieved by folding and uplift of pre-existing large, internal thrust sheets by the continued growth and/or reactivation of duplexes in the hinterland. The growth of a blind imbricate complex off a lower thrust provides another mechanism for folding a higher thrust. Individual splays in a blind imbricate complex may have fault propagation folds and/or fault bend folds associated with them. If the splays reach the overlying thrust, they serve as connecting splays between the lower thrust (floor) and the upper thrust (roof), thereby forming a connecting splay duplex (CSD). This type of duplex geometry requires periodic reactivation of the pre-existing roof thrust.

The Canyon Range thrust in central Utah is an internal thrust that is folded into an overturned antiform–synform pair and overrides its own synorogenic conglomerates. The same conglomerates are infolded into the core of the synform and preserve critical timing information regarding the history of folding and thrust reactivation. The folding is caused by the development of a footwall antiformal stack in the core of the Canyon Range antiformal culmination; the geometry and timing relationships suggest that the structure grew as a CSD. Regional timing relationships suggest that the growth of the CSD and reactivation of the thrust took place during the later part of the evolution of the orogenic wedge, and may have helped the wedge maintain critical taper during thrusting in the external fold-and-thrust belt.

INTRODUCTION

Theoretical models of critically tapered wedges (Davis *et al.*, 1983) provide a useful conceptual framework for interpreting the evolution of fold-and-thrust belts (FTBs). Chapple (1978) first discussed the behavior of a cohesive, ideally plastic wedge in which shortening and thickening spreads from the back to the front of the wedge to create a surface slope (and hence critical taper) to allow the whole wedge to move by sliding on a weak basal plane. Davis *et al.* (1983) and Dahlen (1990) discussed the behavior of non-cohesive frictional Coulomb wedges in which a critical taper must develop by shortening and thickening before the wedge as a whole can move by frictional sliding at its base (Fig. 1a); such wedges may also be thought of as frictional plastic wedges (Mandl, 1988). Although the assumptions regarding material behavior and yield conditions in models of plastic and Coulomb wedges are different, they suggest that all orogenic wedges require the development of taper toward their undeformed foreland, and only advance when the sum (θ) of the basal slope (β) and the surface slope (α) reaches a critical value (θ_c). If the wedge is subcritical ($\theta < \theta_c$) it must shorten and thicken so that θ increases to a critical value. If the wedge is supercritical ($\theta > \theta_c$) it will tend to lengthen itself by propagating thrusts toward the undeformed foreland thereby incorporating parts of a lower taper sedimentary prism into the front of the deformed wedge and reducing θ of the wedge as a whole.

During progressive evolution of an FTB, erosion at the top of the wedge may reduce α, and cause β to decrease as a result of isostatic rebound; thus a wedge may become

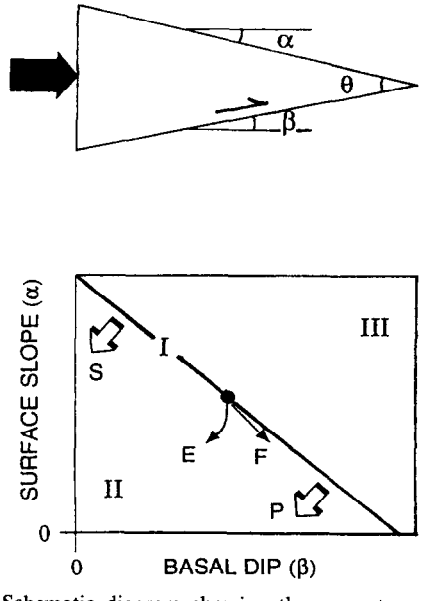

Fig. 1. (a) Schematic diagram showing the geometry of a tapered orogenic wedge. Wedge taper (θ) is the sum of the surface slope (α) and the dip angle of the basal decollement (β). (b) Behavior of a Coulomb wedge in α–β space in response to changes in certain geologic parameters. Labeled fields are: I — Critical, wedge deforms internally and advances in self-similar form; II — Subcritical, wedge stalls due to insufficient taper; III — Supercritical, wedge can slide forward on a single basal thrust. Increased wedge strength (*S*) and increased pore pressure at base (*P*) or decreased basal strength shifts the critical taper line (*I*) downwards. A critically tapered wedge (filled circle) may change its taper as shown as a result of surface erosion (*E*), or flexural subsidence (*F*).

subcritical (Fig. 1b). Another mechanism that causes a wedge to become subcritical is flexural subsidence (Jordan, 1981) which causes α to decrease and β to increase by equal amounts; since β more strongly affects the state of the wedge, it becomes subcritical (Fig. 1b). Whenever a FTB wedge becomes subcritical, internal shortening must take place to reach critical taper before the wedge continues to advance. This implies that internal shortening should occur in the hinterland portion of a FTB wedge throughout thrusting.

Woodward (1987) suggested that there may not be sufficient evidence for the large amounts of continued shortening required in the hinterland. He pointed out that since most FTBs show a hinterland to foreland progression of the initiation of thrusting (Armstrong and Oriel, 1965; Royse *et al.*, 1975; Roeder *et al.*, 1978; Wiltschko and Dorr, 1983; Woodward, 1985) with only minor amounts of break-back thrusting, it seems unlikely that large amounts of late shortening in the hinterland could be accounted for. By assuming that parallel-sided tabular segments of sedimentary rocks were incorporated into the front of the wedge as successive thrusts developed, Woodward (1987) may have significantly overestimated the amount of shortening required in the back of the wedge.

In this paper we first examine the question of how much shortening is required in an originally tapered sedimentary prism to reach critical taper and maintain it during thrusting. Secondly, we look at whether or not there is evidence for such shortening in the back of a wedge throughout thrusting. Finally, we summarize some of the thrusting (duplexing) mechanisms that have been described by others, and we suggest a new duplexing mechanism (based on a well-constrained natural example), that might account for the required shortening in the internal portions of an orogenic wedge.

EFFECT OF SHORTENING STRAIN ON WEDGE TAPER

In a tapered sedimentary prism, the taper angle can be increased by shortening and thickening the prism. In most natural settings the total strain resulting from structures developed at all scales progressively decreases from the back to the front of the wedge (Mitra, 1994), so that the back end is selectively thickened causing the taper angle to increase rapidly. In the following analysis we assume that strain is uniformly distributed through the entire prism, obtaining a maximum estimate of the strain required to enhance taper as it allows thickening both in the back and in the toe of the prism. Assuming plane strain, we can calculate the wedge taper for any given strain if we know what the initial taper of the sedimentary prism was.

We assume a taper angle θ for the initial sedimentary prism of width l and thickness h at its thick end, such that $\tan\theta = h/l$. The taper angle is the same as the basement slope of the sedimentary basin (Fig. 2). As deformation progresses, the wedge is shortened and thickened, thus producing a surface slope toward the foreland. For equal area plane strain ($T_2 = 1$), $T_1T_3 = 1$, i.e. $T_1 = 1/T_3$, where T_1 and T_3 are the vertical and horizontal principal stretches respectively. Because changes in the wedge angle are small, the deformed wedge still approximates a right-angled triangle.The new wedge length $l' = T_3 l = l/T_1$.The new thickness of the wedge at its thick end $h' = T_1 h = h/T_3$.The new taper angle (θ') is given by

$$\tan\theta' = h'/l' = \tan\theta/T_3^2. \quad (1)$$

This simple calculation, based on a small angle approximation, produces essentially the same results as the recent detailed analysis by Boyer (1995). The effects of increasing amounts of strain on the shape of sedimentary wedges of different initial taper are shown in Fig. 2. For example, if a sedimentary prism has an initial taper of 4°, as the wedge is shortened its taper increases along the sloping line; for 30% shortening, taper is increased to 8°. For a particular amount of strain, the taper angle increases by a constant multiplicative factor; thus the absolute enhancement of taper is more pronounced in wedges with high initial taper. For 30% shortening, a 1° initial wedge increases its taper to ~2°, while a 4° initial wedge increases its taper to ~8° (an increase of 4°).

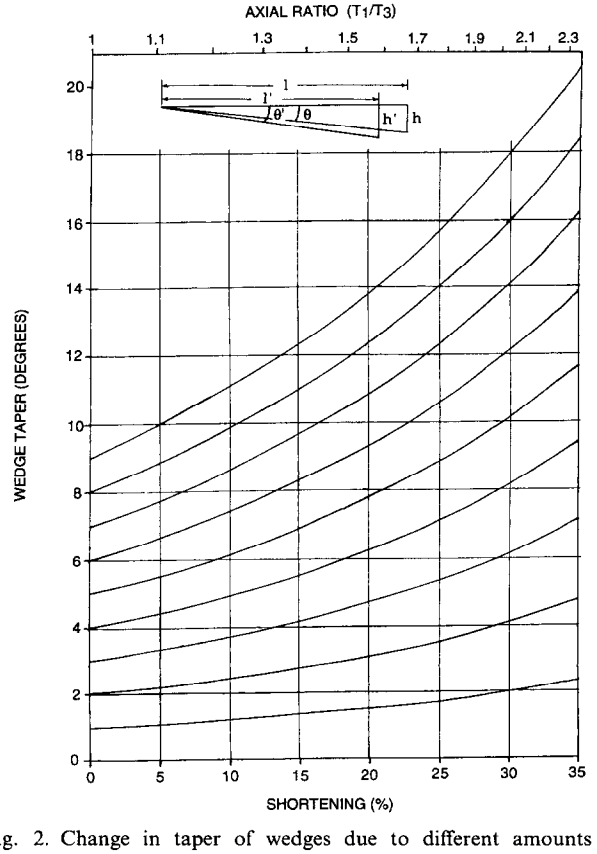

Fig. 2. Change in taper of wedges due to different amounts of shortening strain within the wedge (see text for details).

MECHANISMS FOR THICKENING INTERNAL THRUST SHEETS

Internal thrust sheets in fold-and-thrust belts often show penetrative shortening strains of 30% or somewhat more (Mitra, 1978, 1979, 1994, in press; Ramsay *et al.*, 1983; Ramsay and Huber, 1983; Woodward *et al.*, 1986), although usually these strains occur early in the history of emplacement of the sheets. Penetrative strains generally decrease from the internal to the external parts of a FTB, with external sheets typically showing $<10\%$ shortening. There is growing evidence, however, that internal thrust sheets continue to shorten and thicken by folding and faulting and are progressively uplifted by later lower thrusts that form in the internal portion of the FTB (Schirmer, 1988; Yonkee, 1992); at the same time, thrusting in the external part of the FTB advances onto the foreland (DeCelles, 1994). Internal thick-skinned thrust sheets (i.e. with crystalline basement in the hanging wall) continue to be the dominant source of synorogenic sediments throughout thrusting (DeCelles, 1994; DeCelles and Mitra, 1995; DeCelles *et al.*, 1995). This is active building of structural relief in the rear wedge (made up of rocks with higher strength, such as quartzites and crystalline basement rocks) in order to maintain critical taper in the orogenic wedge as a whole, rather than passive uplift of basement sheets to maintain continuity with advancing external sheets. Effectively, the strong rear wedge drives the weaker sedimentary wedge (with lower taper) in front of it (DeCelles and Mitra, 1995).

Continued thickening in the internal portion of an orogenic belt can take place by a variety of mechanisms depending on the conditions of deformation. These might include (1) penetrative bulk shortening at high metamorphic grades; (2) folding and fold-tightening in layered rocks deforming at low to high metamorphic grades; and (3) faulting, manifested particularly by duplexing of various kinds, that might continue to be active in the internal portion of a FTB, generally at low metamorphic grades. Here we focus on the duplexing mechanisms that thicken the internal portion of an orogenic wedge during deformation; these include (1) basement duplexing, (2) reactivation of internal duplexes, and (3) connecting splay duplexing.

BASEMENT DUPLEXES

Thick-skinned thrust slices carrying crystalline basement are common in the external-to-internal transition zones of most orogenic belts (Royse *et al.*, 1975; Harris, 1978; Mitra, 1979; Mitra and Elliott, 1980; Bruhn and Beck, 1981; Boyer and Elliott, 1982; Roeder, 1989; Yonkee, 1992; Rodgers, 1995). In many cases, these basement slices show internal repetition by thrusting, forming duplexes or antiformal stacks (Elliott and Johnson, 1980; Boyer and Elliott, 1982; Stanley and Ratcliffe, 1983; Coward and Butler, 1985; Schirmer, 1988; Schonborn, 1992; Yonkee, 1992). Recent work on timing of faults within these duplexes suggests that while the earliest thrust in the duplex generally forms before thrusting advances into the external thrust belt, the basement duplex continues to grow progressively even as thrusting in the sedimentary section propagates forelandward (Schonborn, 1992; DeCelles, 1994). In fact, there is a direct relationship between growth of a basement duplex in the internal portion of the FTB and thrusting in the external part of the belt (DeCelles and Mitra, 1995).

In the Sevier FTB in NE Utah, the Farmington Canyon Complex is made up of the Ogden duplex which contains several horses of strongly deformed Precambrian crystalline basement that form an antiformal stack (Schirmer, 1988; Yonkee, 1992; Yonkee and Mitra, 1993). This structure constitutes the doubly-plunging Wasatch culmination, which forms the leading edge of a strong, thick rear wedge with high taper. Timing information obtained from intersection relationships of thrust faults and related folds, regional angular unconformities, and ages and provenance of synorogenic deposits suggest that the emplacement of successive basement thrust slices in the culmination are temporally related to movement on successive major thrusts in the external portion of the FTB (Fig. 3a; DeCelles, 1994). Emplacement of successive basement slices within the Ogden duplex provides the taper enhancement needed at each stage for thrusting to progress on to the foreland in the thinner, weaker, low-taper sedimentary wedge (DeCelles and Mitra, 1995). Erosion of the wedge-top typically keeps up with tectonic activity, but eventually outpaces uplift and lowers the taper so that the wedge becomes subcritical; taper is then enhanced again by emplacement of the next basement slice, and the process is repeated (DeCelles, 1994; DeCelles and Mitra, 1995).

A very similar tectonic history has been described from the Central Southern Alps (Schonborn, 1992). There, the emplacement of successive basement slices in a duplex culmination in the internal portion of the fold-and-thrust belt is directly related to southward directed thrusting in the external part of the FTB (Fig. 3b). In this case, the duplex is described to have a break-back sequence within it with one of the slices being emplaced out-of-sequence (Schonborn, 1992); but, an alternative explanation may be that one of the basement slices was reactivated during duplex development.

In the Blue Ridge province of the Southern Appalachians in North Carolina–Tennessee, balanced cross-sections indicate the presence of a two-tiered duplex (Boyer and Elliott, 1982). The upper duplex, made up of slices of Precambrian basement and Proterozoic cover, folded the overlying Blue Ridge thrust sheet (made up of Precambrian crystalline basement rocks) during the Acadian and/or Alleghanian orogeny (Boyer, 1992a); concurrently the first thrusts were emplaced in the Valley and Ridge province (Fig. 3c). During the main part of

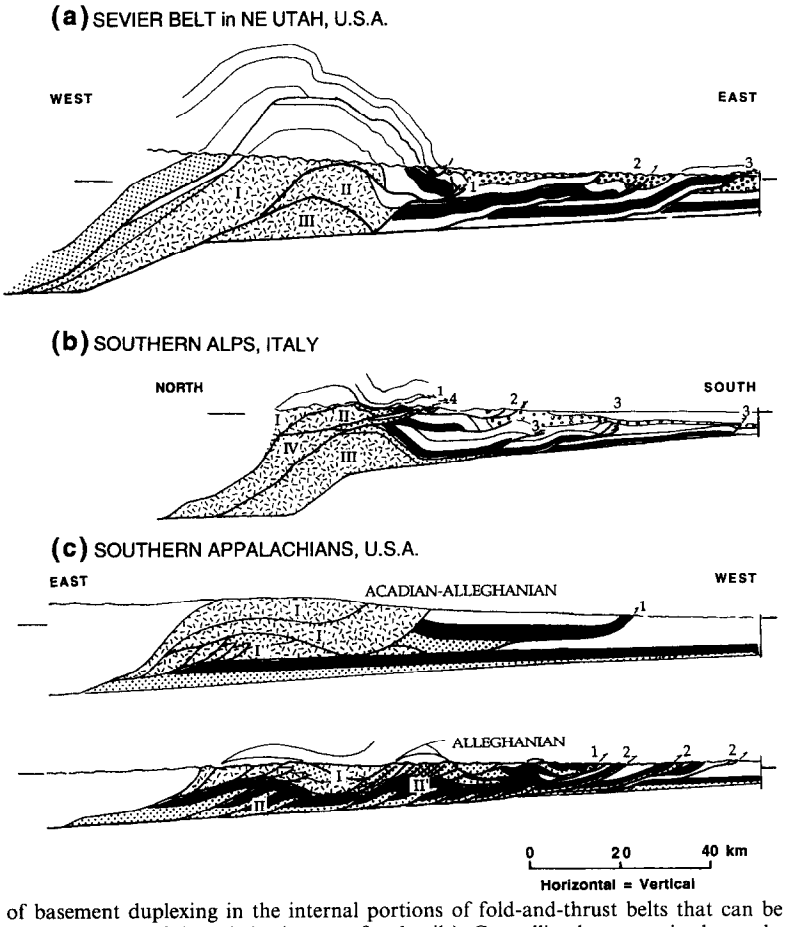

Fig. 3. Examples of basement duplexing in the internal portions of fold-and-thrust belts that can be directly related to thrusting in the external portions of those belts (see text for details). Crystalline basement in thrust sheets are shown with 'granite' pattern, and synorogenic sedimentary rocks with open circle pattern. Successive basement slices are labeled I, II, III ... etc., while corresponding external cover thrust sheets are labeled 1, 2, 3 ... etc.

the Alleghanian orogeny the basement duplex was uplifted over a duplex that developed in Cambro-Ordovician sedimentary rocks (Boyer, 1992a), and at the same time deformation progressed toward the foreland forming the remaining thrusts of the Valley and Ridge province (Fig. 3c). Clearly, the continued uplift and thickening of the internal, thick-skinned portion of the thrust belt helped maintain taper as thrusting advanced on to the foreland.

REACTIVATION OF INTERNAL DUPLEXES

Boyer (1992b) proposed a model by which the imbricate faults in the back of a typical duplex (Boyer and Elliott, 1982) continue to be active even after frontal faults in the duplex have developed. Generally, the imbricate faults in a duplex grow successively from the back to the front of the duplex, and it is assumed that movement on older faults is shut off (older slices are carried piggy-back) as younger faults develop. If an older imbricate fault I in a duplex continues to be active after a younger imbricate II has developed, slip on I is transferred to the roof thrust, and hence to the front of the duplex (Fig. 4a, after Boyer, 1992b). This leads to

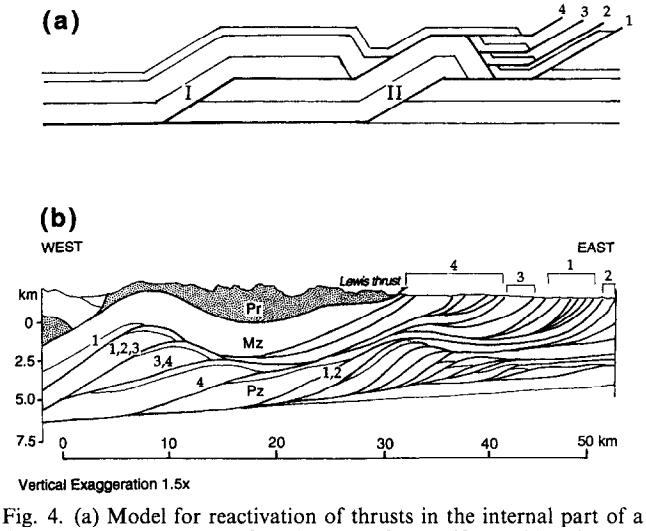

Fig. 4. (a) Model for reactivation of thrusts in the internal part of a duplex (Boyer, 1992b). After thrust II forms, if an older thrust I continues to be active it gives rise to synformally folded imbricates in a break-back sequence (1, 2, 3, 4) above the roof thrust and in front of the ramp anticline associated with thrust II. (b) The sub-Lewis duplex and the Waterton gas-fields duplex in southern Alberta showing the synformally folded imbricate thrusts above and in front of the duplexes. Sequential timing of fault motions is shown by the numbers 1,2, ... etc. Balanced restorations (Boyer, 1992b) suggest that the imbricate thrusts formed in the order shown (i.e. 1, 2, 3, 4), and faults within the underlying duplexes were (repeatedly) reactivated during the formation of successive imbricates.

imbrication off the crest of the frontal anticline of the duplex, where the roof thrust is folded over the ramp in II, following Gilluly's model (Gilluly, 1960) of simultaneous thrusting and folding (Fig. 4a). The resulting structure has a series of break-back imbricates in the core of the syncline that lies immediately in front of the frontal anticline of the duplex. If the main duplex structure continues to grow, it results in a series of break-back imbricate fans, leading to a complex structural geometry and kinematic history; an excellent example is provided by the Sub-Lewis duplex in the Waterton gas-fields of the southern Canadian Rockies (Fig. 4b, after Boyer, 1992b). A number of other well-known duplexes exhibit similar imbricate geometries suggesting development by synchronous folding and thrusting (Boyer, 1992b); the structures are difficult to explain as the result of folding of pre-existing imbricate fans.

Continued activity on faults in the back of a duplex leads to larger total displacements on early faults and repetition of the stiff members that make up the duplex, and hence to continued thickening in the back. The thickening helps build structural elevation at the back of the duplex and maintain taper in the orogenic wedge as a whole, driving thrusting in the higher stratigraphic package that lies farther toward the foreland. Most of the examples cited by Boyer (1992b) are developed in sedimentary rocks, but similar reactivation of older thrusts in a duplex may also occur in thick-skinned duplexes carrying crystalline basement rocks; the kinematic history determined for the basement duplex in the internal portion of the Southern Alps (Schonborn, 1992; Fig. 3b) provides one possible example.

CONNECTING SPLAY DUPLEXES

If there is continuing activity in the internal portion of a FTB, even as thrusting progresses toward the external portion of the belt, *blind imbricates* (Woodward *et al.*, 1989) and *connecting splays* (Boyer and Elliott, 1982) may form between pre-existing thrusts in the internal FTB (Fig. 5). A blind imbricate fan off a reactivated lower thrust will result in folding of a higher thrust (Fig. 5). Connecting splays join two pre-existing thrusts (Fig. 6); two or more such connecting splays that form between two pre-existing thrusts will give rise to a Connecting Splay Duplex (CSD). Unlike a typical duplex (Boyer and Elliott, 1982) in which the floor thrust grows progressively as the duplex develops, a CSD has pre-existing floor and roof thrusts. Reactivation of a pre-existing floor thrust may induce formation of a connecting splay, allowing slip to transfer to a pre-existing roof thrust, thus reactivating it. Thus, timing information indicating that both the floor and roof thrusts were present, and that they were both reactivated at the time of formation of the connecting splays, is critical to recognizing this type of duplexing. Geometrically, connecting splay duplexes (Fig. 5) look very similar to typical duplexes described by Boyer and Elliott (1982), and, in the absence of good

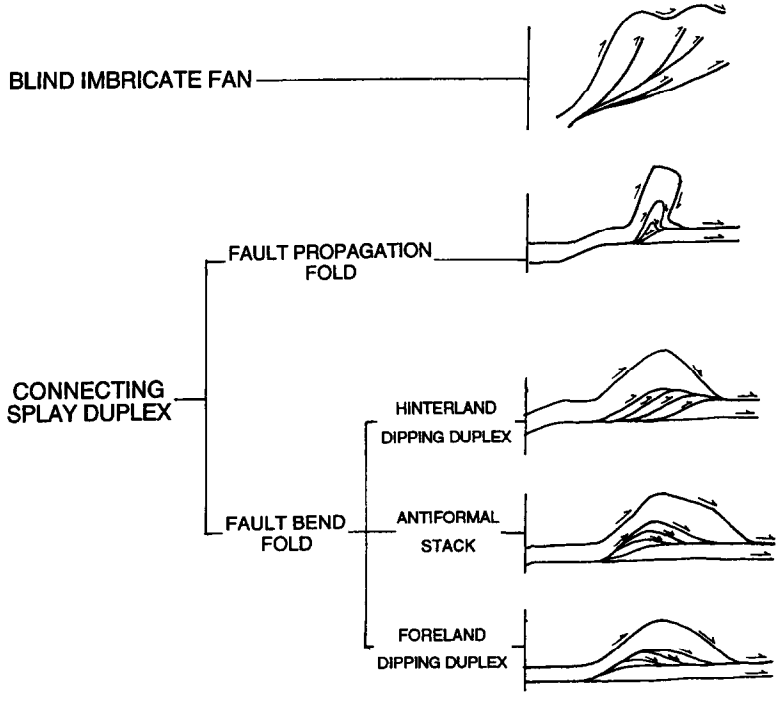

Fig. 5. Classification of different types of late-stage imbricate fault systems that may propagate off a lower thrust and result in folding of an older, upper thrust. If the blind imbricates reach the upper thrust they give rise to different types of connecting splay duplexes.

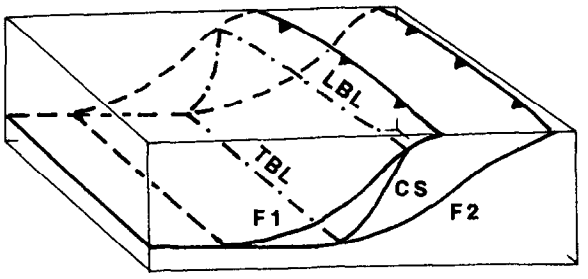

Fig. 6. The geometry of a connecting splay (CS) between two pre-existing thrusts (F1 and F2). The trailing branch line (TBL) and leading branch line (LBL) of the connecting splay are shown.

timing information, they may not be easily recognized. We present models of possible CSD geometries that may develop when individual horses are folded by fault bend folding or fault propagation folding.

Fault bend fold connecting splay duplexes

Emplacement of successive connecting splays between pre-existing floor and roof thrusts results in a CSD that uplifts the upper sheet forming an antiformal structure. If successive slices are deformed by fault bend folding, then depending on the magnitude of slip on the individual connecting splays compared to the original spacing between them, the CSDs could be hinterland-dipping, foreland-dipping or form an antiformal stack similar to typical duplexes (Boyer and Elliott, 1982; Mitra and Boyer, 1986). The antiform in the upper sheet gets broader (greater wavelength) as successive horses are emplaced in either a hinterland-dipping (Fig. 7a) or a foreland-dipping (Fig. 7b) CSD. For an antiformal stack CSD, the fold amplitude progressively increases as successive slices are emplaced (Fig. 8a); if the higher slices are continually deformed as lower slices are emplaced there may be some thinning in the limbs of the fold (Fig. 8b). In all cases, the resulting fold in the upper sheet tends to be upright. Also, a lower thrust (the pre-existing floor thrust) always lies below and in front of the duplex. For fault bend folding of the slices to take place, large amounts of slip have to be transferred from the floor to the roof thrust. Thus the roof thrust should show evidence for significant reactivation, with large amounts of additional slip taking place on the thrust after its initial emplacement. Although we have found no well-documented examples of these structures due to the lack of detailed timing information, we would expect them to be present in the internal portions of FTBs.

Fault propagation fold connecting splay duplex

This structure develops in a manner similar to a blind imbricate complex (Woodward *et al.*, 1989), where an imbricate fan develops off a lower thrust and results in folding of the upper thrust (Fig. 5) (Lamerson, 1982). Each of the faults in a blind imbricate fan has a tip-line (i.e. the fault dies out) within the core of the large fold, and each may have a tip anticline (fault propagation fold) associated with it which folds the upper fault. If an individual imbricate breaks through the structure to reach the upper fault, a small amount of slip is transferred to it (Fig. 9). The resulting fold in the upper sheet is tighter than in fault bend folding, and has a steep forelimb. As successive imbricates reach the upper thrust the overall structure evolves into a CSD with a roof thrust (the upper folded thrust), a floor thrust from which the imbricates originate, and connecting splays (the imbricate faults) that join the floor and the roof. If the individual imbricate slices form an antiformal stack, the resulting antiform in the upper sheet has large structural elevation, a steep to overturned forelimb that is stretched and thinned, and a tight to isoclinal adjoining synform in front of it. During the growth of this structure the roof thrust is periodically reactivated as each slice is emplaced under it, and a small amount of additional slip occurs on the roof thrust at each stage (Fig. 9).

As in any imbricate fan the imbrication is typically localized at some pre-existing structure such as a ramp in the lower thrust, which may already have a fault bend fold associated with it. The folding caused by the CSD helps to tighten the pre-existing fold if the successive slices emplaced into the core of the fold are progressively smaller. The resulting antiformal stack has a distinctive geometry with smaller slices lower down in the structure; this is not always the case in the type of antiformal stacks described by Boyer and Elliott (1982) (e.g. Mitra, 1986).

We suggest that when slip is being transferred from the imbricate thrust to the roof thrust, the leading branch line (LBL) for each imbricate should lie at the synformal hinge (Fig. 10) so that the upper sheet does not have to be transported through the synformal hinge. During emplacement of the second imbricate, fault propagation folding at its tip will cause the first slice to be folded, thereby tightening the fold in the upper sheet and also causing the synformal hinge to shift forelandward from the first leading branch line (LBL1). Thus, the leading branch line of the second imbricate (LBL2), which should be at the second stage synformal hinge, will lie farther toward the foreland than LBL1 (Fig. 10). Successive connecting splays join the roof thrust farther toward the foreland, and earlier leading branch lines are uplifted to a higher structural elevation in the steep common limb of the antiform–synform pair (Fig. 10).

The geometry of connecting splay duplexes is similar in many ways to other duplexes, and timing information is necessary for recognizing these structures. We present a well-constrained example from the Canyon Range in central Utah where we have been able to determine the kinematic history of a fault propagation fold CSD on the basis of regional and local timing information, structural geometry, and microstructural data. Because CSDs have not been described before, we present this case study here in considerable detail.

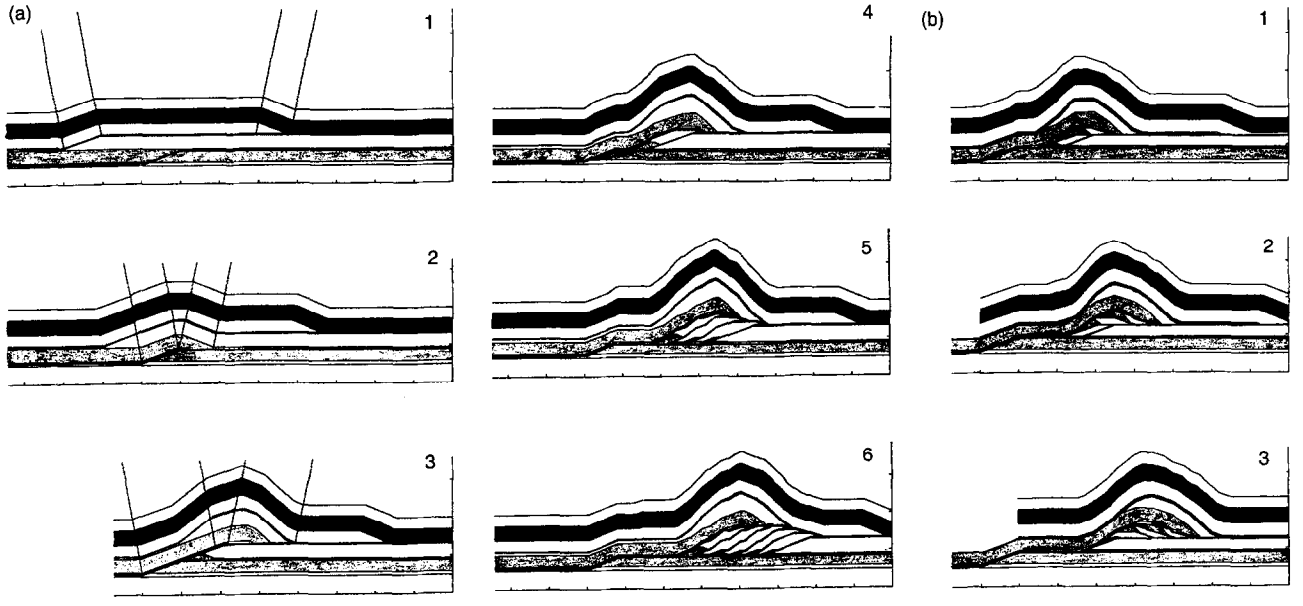

Fig. 7. (a) Growth of a connecting splay duplex by fault bend folding. After initial emplacement (1) and folding (2) of a thrust by an underlying thrust, a connecting splay forms at the lower ramp (3). Succeding connecting splays may form a hinterland dipping duplex, shown after the formation of one (4), three (5) and five (6) horses. The upper thrust sheet is folded into an upright anticline whose maximum amplitude is above the first two horses, and remains there even as the duplex develops into its typical flat-topped form. (b) After an initial history similar to (a), the connecting splays form a foreland dipping duplex. The resulting folding of the upper sheet has a geometry very similar to that in (a).

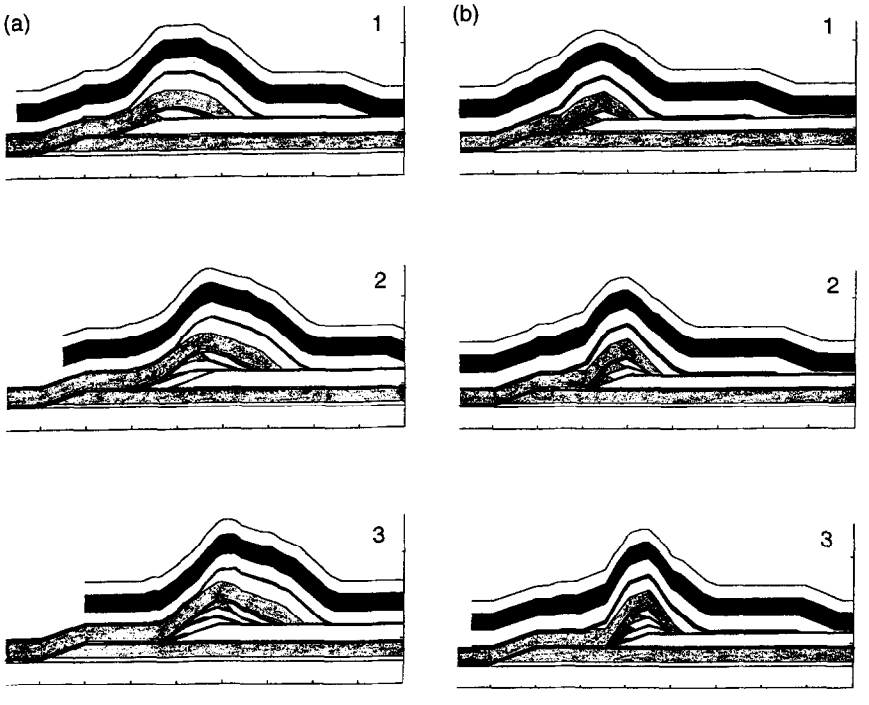

Fig. 8. (a) After an initial history similar to that shown in Fig. 6(a), connecting splays form an antiformal stack by parallel folding. The upper sheet is folded into a broad, upright anticline. (b) The connecting splay antiformal stack may form by superposing trailing branch lines if there is some thinning in the limbs of the older horses. The resulting anticline in the upper sheet is somewhat narrower and more steep-sided.

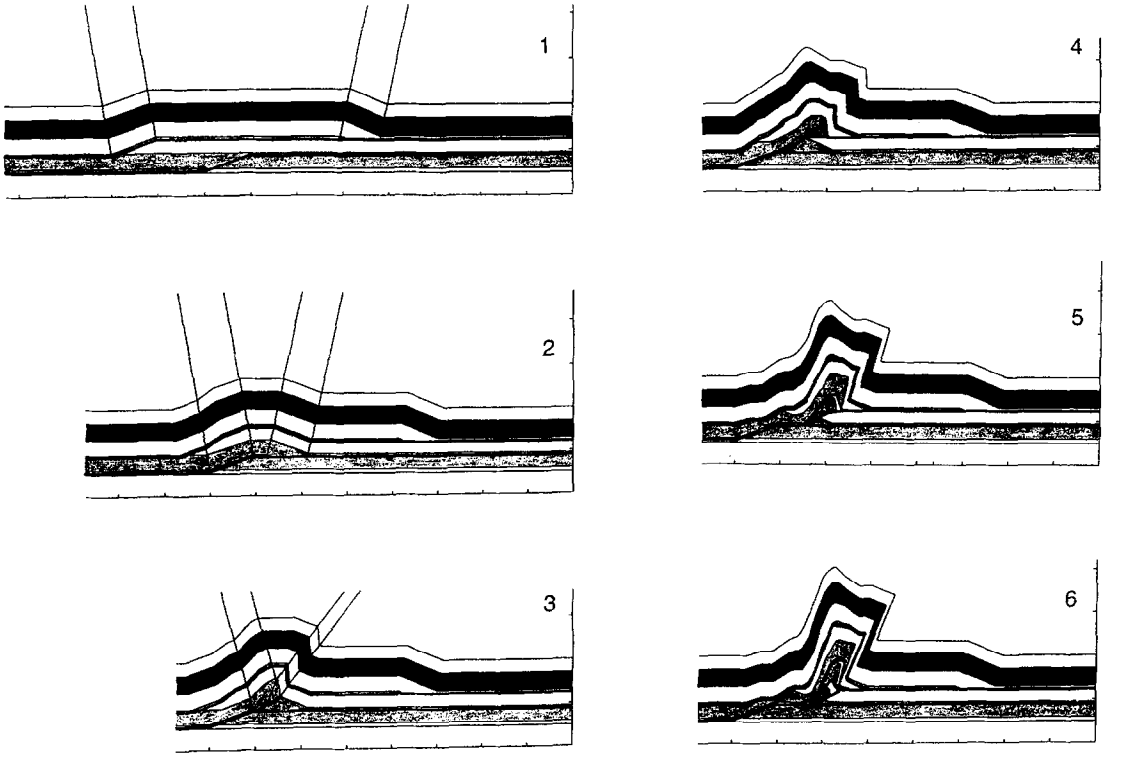

Fig. 9. Growth of a connecting splay duplex by fault-propagation folding. After initial emplacement (1) and folding (2) of a thrust by an underlying thrust, an imbricate starts to form at the lower ramp with a fault propagation fold at its tip (3). The imbricate eventually joins the roof thrust, transferring a small amount of slip to the roof (4). A similar progression is followed by succeding imbricates (5, 6). The upper thrust sheet is folded into a steep-sided, overturned anticline with considerable thinning in its forelimb, and an adjoining tight syncline.

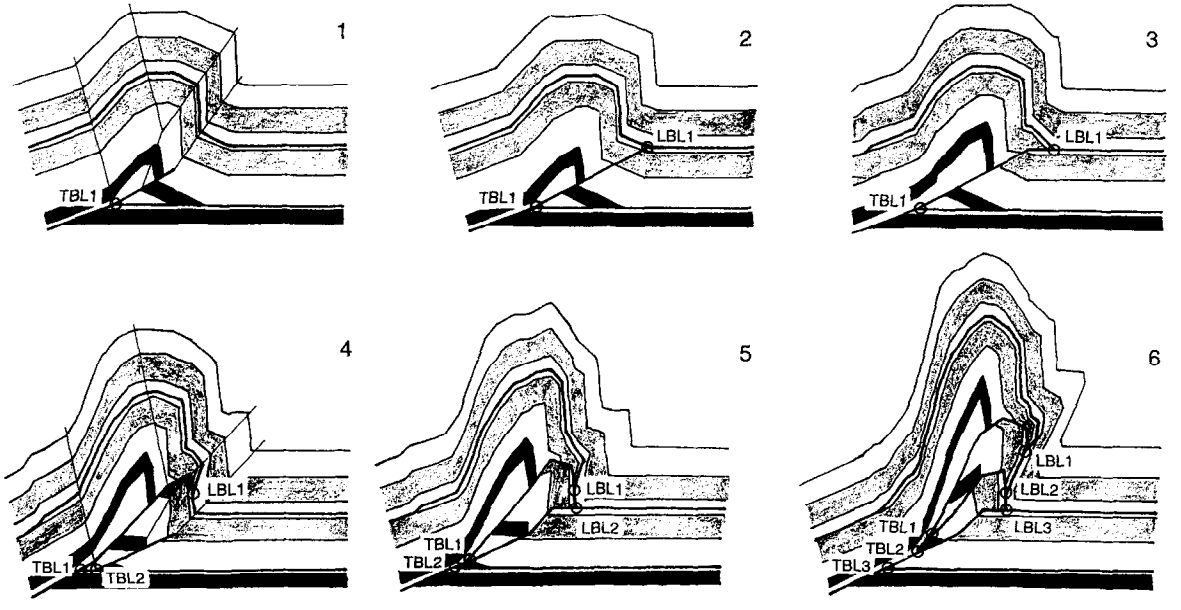

Fig. 10. Growth of successive connecting splays during the formation of a fault propagation fold duplex. The first connecting splay (1) reaches the roof at the synformal hinge (LBL1 in 2) and is displaced forward along the upper flat (3). During growth of the second imbricate (4), LBL1 moves into the forelimb of the antiform as the fault propagation fold grows. The imbricate reaches the roof at the synformal hinge (LBL2 in 5) forelandward of LBL1, and is displaced forward along the upper flat. LBL2 is, in turn, rolled into the forelimb as the fault propagation fold grows with the third imbricate, with this fault also eventually reaching the roof (6).

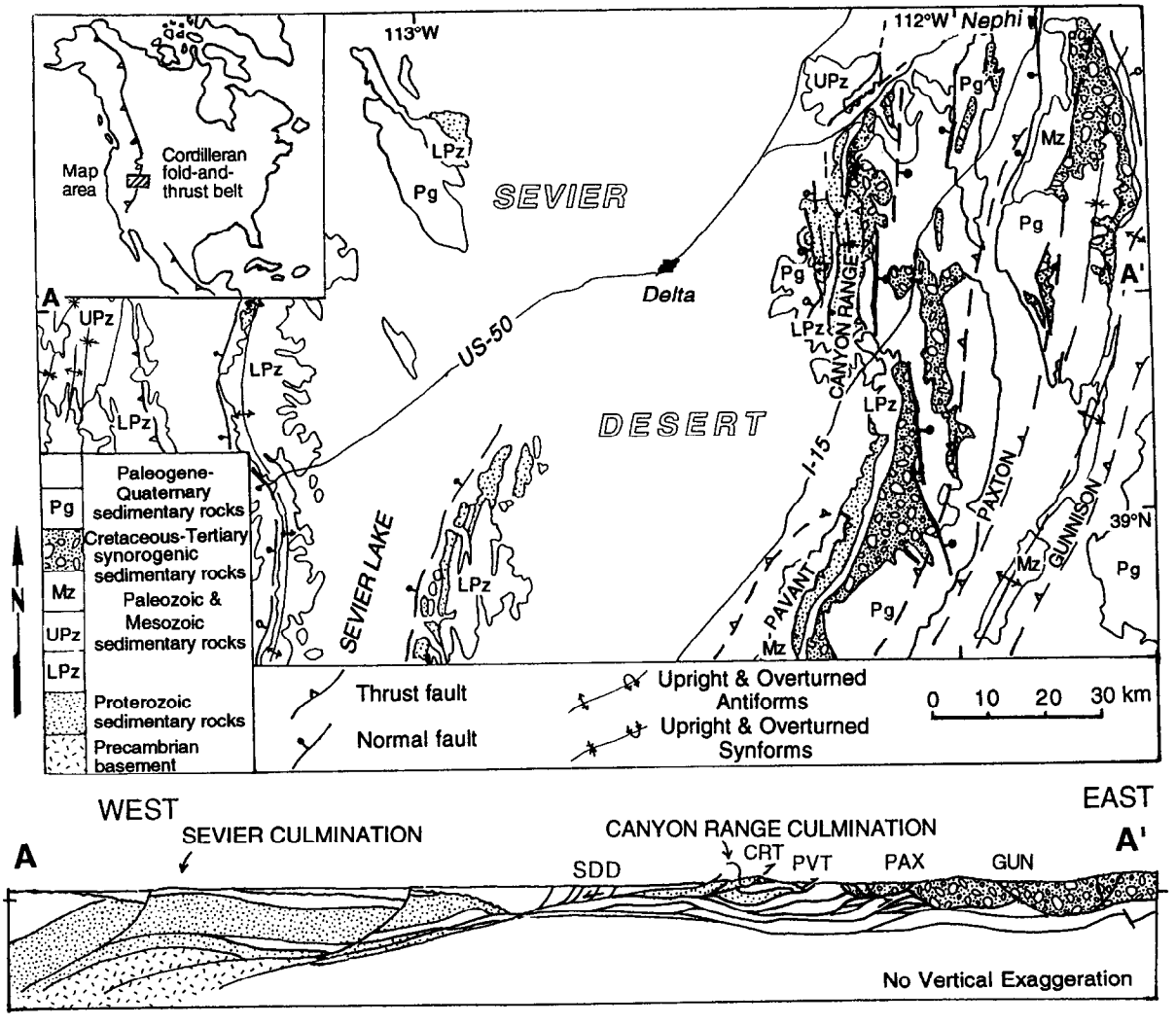

Fig. 11. Generalized geologic map of central Utah showing the major Sevier-age structures exposed in the ranges of the Basin-and-Range province (after Hintze, 1980). Location of map in Fig. 13 is shown. Line of regional cross-section (AA') is also shown. The cross-section along AA' (after Coogan *et al.*, 1995) shows the major structures: Sevier culmination, Canyon Range culmination, CRT — Canyon Range thrust, PVT — Pavant thrust, PAX — Paxton thrust, GUN — Gunnison thrust, DD — Sevier Desert detachment fault.

The Canyon Range connecting splay duplex

Regional geology. The Sevier fold-and-thrust belt (FTB) defines the eastern margin of thin-skinned deformation in the Cordilleran orogen of western North America (Fig. 11) (Armstrong, 1968; Burchfiel and Davis, 1975; Allmendinger, 1992; Miller *et al.*, 1992). In this belt, Proterozoic, Paleozoic and Mesozoic miogeoclinal rocks were transported eastward during the late Cretaceous (55–140 Ma) Sevier orogeny (Armstrong, 1968; Burchfiel and Davis, 1975; Schwartz and DeCelles, 1988). The central Utah segment (Fig. 11) of the Sevier fold-and-thrust belt (FTB) has four major thrusts: they are (from west to east) the Canyon Range, Pavant, Paxton and Gunnison thrusts (Christiansen, 1952; Armstrong, 1968; Burchfiel and Hickcox, 1972; Higgins, 1982; Lawton, 1982, 1985; Standlee, 1982; Allmendinger *et al.*, 1983; Holladay, 1983; Millard, 1983; Villien and Kligfield, 1986; Royse, 1993; Mitra *et al.*, 1994, 1995; Pequera *et al.*, 1994; Coogan *et al.*, 1995; DeCelles *et al.*, 1995; Sussman, 1995; Sussman and Mitra, 1995a,b). The thrusts sheets are broken up by Tertiary Basin-and-Range normal faulting (Fig. 11). The internal thrust sheets (Canyon Range and Pavant) have Proterozoic through Lower Paleozoic rocks preserved in their hanging walls (Fig. 11). The external thrusts were blind, and have also been covered by later sediments; their structure is known mainly from subsurface (seismic and drill-hole) information (Fig. 11; Standlee, 1982; Coogan *et al.*, 1995).

Tectonic evolution of this part of the Sevier FTB is constrained on the basis of stratigraphic and provenance information from both distal (east) and proximal (west) Cretaceous synorogenic sediments (Fig. 12). Initial emplacement of the Canyon Range thrust sheet took place during Neocomian time (~120–140 Ma) (DeCelles *et al.*, 1995); the Cedar Mountain Formation (120–130 Ma), containing clasts derived from the Canyon

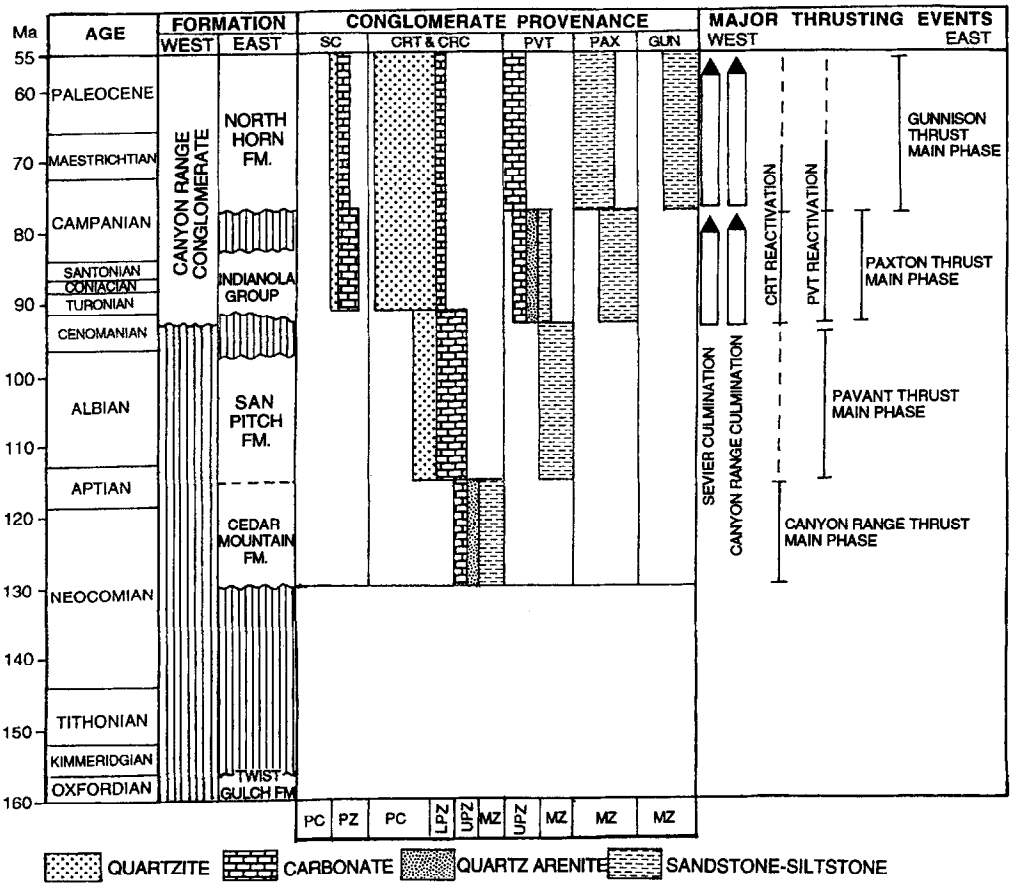

Fig. 12. Chart showing provenance of Cretaceous–Paleocene synorogenic deposits and sequential timing of thrust faulting in the central Utah segment of the Sevier FTB. Source areas for conglomerate clasts are shown along the top of the chart: Sevier culmination (SC), Canyon Range thrust sheet and Canyon Range culmination (CRT & CRC), Pavant sheet (PVT), Paxton sheet (PAX) and Gunnison sheet (GUN). Likely source stratigraphic units for the synorogenic deposits are shown by ages along the bottom of the chart. (Based on DeCelles *et al.*, 1995.)

Range sheet were deposited during this time (Yingling and Heller, 1992; DeCelles *et al.*, 1995; Currie, in press). Initial Pavant thrusting is recorded by synorogenic deposits of the late Aptian to Albian (110–115 Ma) San Pitch Formation or upper Pigeon Creek Formation (Schwans, 1988; Sprinkel *et al.*, 1992) which contains clasts derived from the Pavant and Canyon Range sheets (DeCelles *et al.*, 1995). The main phase of Paxton thrusting was from Cenomanian to Campanian time (80–95 Ma), during which Indianola Group sediments were shed from the orogen; the presence of Proterozoic quartzite clasts in the Indianola suggests reactivation of the Canyon Range and Pavant thrusts (DeCelles *et al.*, 1995) and growth of a culmination in the Canyon Range at this time (Sussman, 1995; Sussman and Mitra, 1995a,b). Clast compositions in the contemporaneous proximal lower Canyon Range conglomerates (Fig. 12) indicate growth of the basement-cored Sevier culmination in the hinterland and folding and fold-tightening of the Canyon Range sheet, growth of the Canyon Range culmination and eventual erosional breaching of the antiformal stack in the footwall of the Canyon Range thrust (Figs 11 & 12; DeCelles *et al.*, 1995; Sussman and Mitra, 1995a,b). Gunnison thrusting took place in Campanian through Paleocene time (55–75 Ma) (Fig. 12) as indicated by progressive deformation in North Horn strata (55–75 Ma) (Lawton, 1985) along the frontal triangle zone of the thrust (Talling *et al.*, 1994; DeCelles *et al.*, 1995). The North Horn Formation and contemporaneous upper Canyon Range conglomerates contain

Fig. 13. Geologic map of the Canyon Range showing the major structural elements and representative bedding dips. The Canyon Range thrust (CRT) Carries Proterozoic–Cambrian rocks in its hanging wall and is folded into a syncline; the CRT overrides its own synorogenic deposits on the east limb of the syncline. The thrust is east-dipping to overturned (west-dipping) on the western limb of the syncline. Cambrian footwall rocks are exposed in the core of the adjoining anticline, truncated by Tertiary normal faults on the west side of the range. The Tintic Valley thrust (TVT) branches from the CRT at the northern end of the Range. Lines of cross-section (XX′, YY′, ZZ′) through the syncline, and down-plunge projections (BB′, CC′) through the antiformal stack are shown. Stratigraphic units shown are: pCp — Proterozoic Pocatello Formation, pCc — Proterozoic Caddy Canyon Formation, pCm — Proterozoic Mutal Formation, Ct — Cambrian Tintic Formation, Cc — Cambrian carbonate rocks, O — Ordovician, S — Silurian, D — Devonian, Mh — Mississippian Humbug Formation, PPo — Pennsylvanian—Permian Oquirrh Formation, TKc — Cretaceous–Tertiary conglomerates, Toc — Tertiary Oak City Formation.

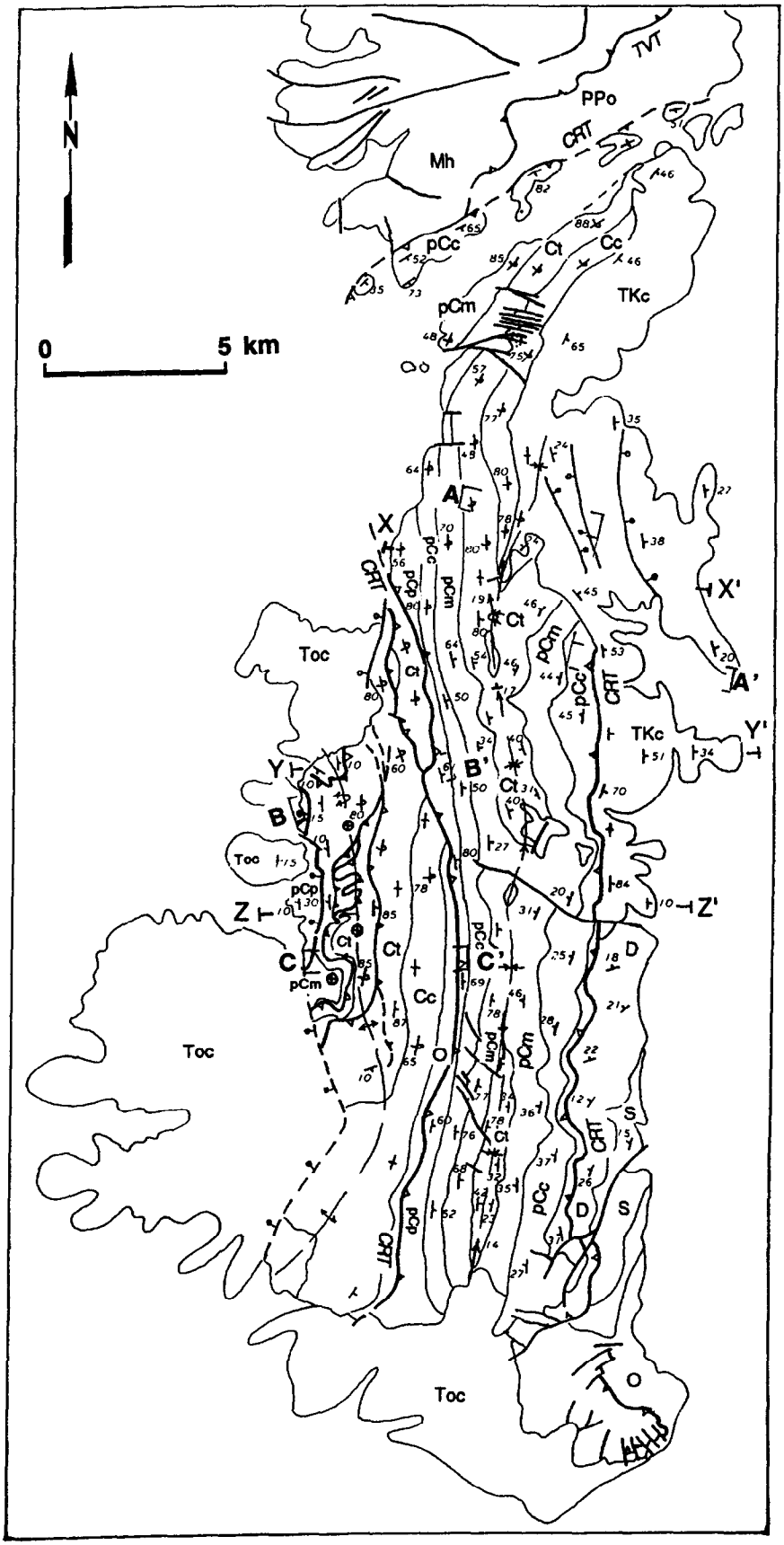
N
0
5 km
TVT
PPo
CRT
Mh
pCc
Ct
Cc
TKc
pCm
Toc
pCp
A
A'
B
B'
C
C'
D
S
O
X
X'
Y
Y'
Z
Z'

Proterozoic–Cambrian quartzite clasts derived from the Canyon Range culmination which continued to be active.

Most of the synorogenic sediments were derived from internal thrust sheets (Canyon Range and Pavant) which continued to be active through the entire period of thrusting and were uplifted as the Canyon Range culmination grew (Fig. 11). Proterozoic and Cambrian quartzite clasts are present through much of the synorogenic sedimentary section. The Proterozoic quartzite clasts could only have been derived from the Canyon Range, since the Proterozoic rocks farther to the west (Sevier culmination) have a preserved Paleozoic cover and were thus never exposed at the surface (Fig. 11). Thus, understanding the structural and kinematic evolution of the Canyon Range thrust sheet and its footwall is the key to understanding the kinematic evolution of this segment of the Sevier FTB wedge.

Structural geology of the Canyon Range. The first order structures exposed in the Canyon Range in central Utah are: (1) a large syncline that has folded the Canyon Range thrust sheet, that is exposed in the middle and eastern part of the range (Christiansen, 1952); and (2) a corresponding antiformal structure along the western flank of the range that is truncated by Tertiary normal faults and only partially exposed (Christiansen, 1952; Holladay, 1983) (Fig. 13).

The synclinal trace runs N–S along the middle of the range for much of its length, but bends to the NE at the northern end (Fig. 13). The fold hinge is horizontal to variably plunging to the north or south; in the northern half of the range the fold plunges northward, with the plunge angle progressively increasing northward to a maximum of ~45°. In the east limb of the syncline, the Canyon Range thrust dips 30–40° westward and places Upper Proterozoic quartzites on top of Devonian carbonates and Cretaceous synorogenic conglomerates. In the west limb of the syncline, the folded Canyon Range thrust generally dips eastward and places Middle Proterozoic quartzites on top of Cambrian quartzites and carbonates, indicating that the thrust climbs through the stratigraphic section in its transport direction in both the hanging wall and the footwall. The syncline progressively tightens toward the north, and changes from an upright to an overturned fold; the thrust dip in the west limb varies accordingly, with the thrust getting progressively steeper northward and eventually becoming overturned at the northern end of the range (Fig. 14).

The steep to overturned beds that form the west limb of the syncline are part of the common limb with an adjoining antiformal structure exposed along the western flank of the range (Fig. 13). Erosion has breached the core of the antiform revealing footwall rocks in a half-window structure; the western half of the window is truncated by Tertiary normal faults associated with Basin and Range deformation (Fig. 13; Otton, 1995). In the footwall, the Upper Proterozoic–Lower Paleozoic section is repeated on a series of imbricate thrusts which form an antiformal stack (Sussman, 1995; Sussman and Mitra, 1995a,b, in review). Fault and bedding dips within the thrust slices define an antiformal pattern, varying from steeply dipping to the east to overturned westward in the eastern part of the window, through horizontal in the middle, to gently westward-dipping in the western-most exposed parts of the window (Figs 13 & 15). The imbricate slices are laterally discontinuous and overlap one another like fish-scales; thus, even though a total of 7 imbricate slices have been mapped, down-plunge projections reveal that on any given transport-parallel line of cross-section the antiformal stack is made up of 3 or 4 horses (Fig. 15b & c). On the northern cross-section (Fig. 15b), the uppermost slice shows a leading branch-line with the Canyon Range thrust which forms the roof of the antiformal stack. The imbricate faults come off the next lower thrust, the Pavant thrust, which forms the floor of the structure.

The geometric attributes of the duplex structure, on the basis of detailed field mapping and down-plunge projections (Sussman, 1995; Sussman and Mitra, 1995a,b, in review), include:

(1) a tight antiform with large structural relief,

(2) steep to overturned forelimb with vertical stretching and thinning,

(3) leading branch-lines with pre-existing roof thrust and

(4) a very tight syncline in front of the duplex.

All these characteristics agree with the model for a connecting splay duplex formed by fault propagation folding (Fig. 9).

Timing of thrusting and folding. Tightly folded Cretaceous synorogenic Canyon Range conglomerates are preserved in the core of the syncline, and overlie Cambrian quartzites and carbonates along a folded erosion surface (Fig. 15a). Different conglomerate units have been mapped on the basis of the composition of clasts present within them (DeCelles *et al.*, 1995). Individual conglomerate units can be traced from the core of the syncline to the eastern flank of the range where they are overridden by the Canyon Range thrust sheet (Christiansen, 1952). We used angular unconformities between conglomerate units, present on both limbs of the syncline, to step-wise unfold the syncline (Fig. 16) following a procedure similar to DeCelles *et al.* (1991). This unfolding indicates that at the time of first conglomerate deposition the fold interlimb angle was 156°, and the thrust sheet had been eroded down to the level of the Cambrian rocks. Progressive tightening of the fold took place mainly by rotation of the west limb to a present-day interlimb angle of 33°. The fold tightening took place under a shallow (<2 km) overburden of synorogenic deposits; populations of brittle fractures and faults present only in the west limb of the syncline indicate E–W shortening and vertical stretching on a

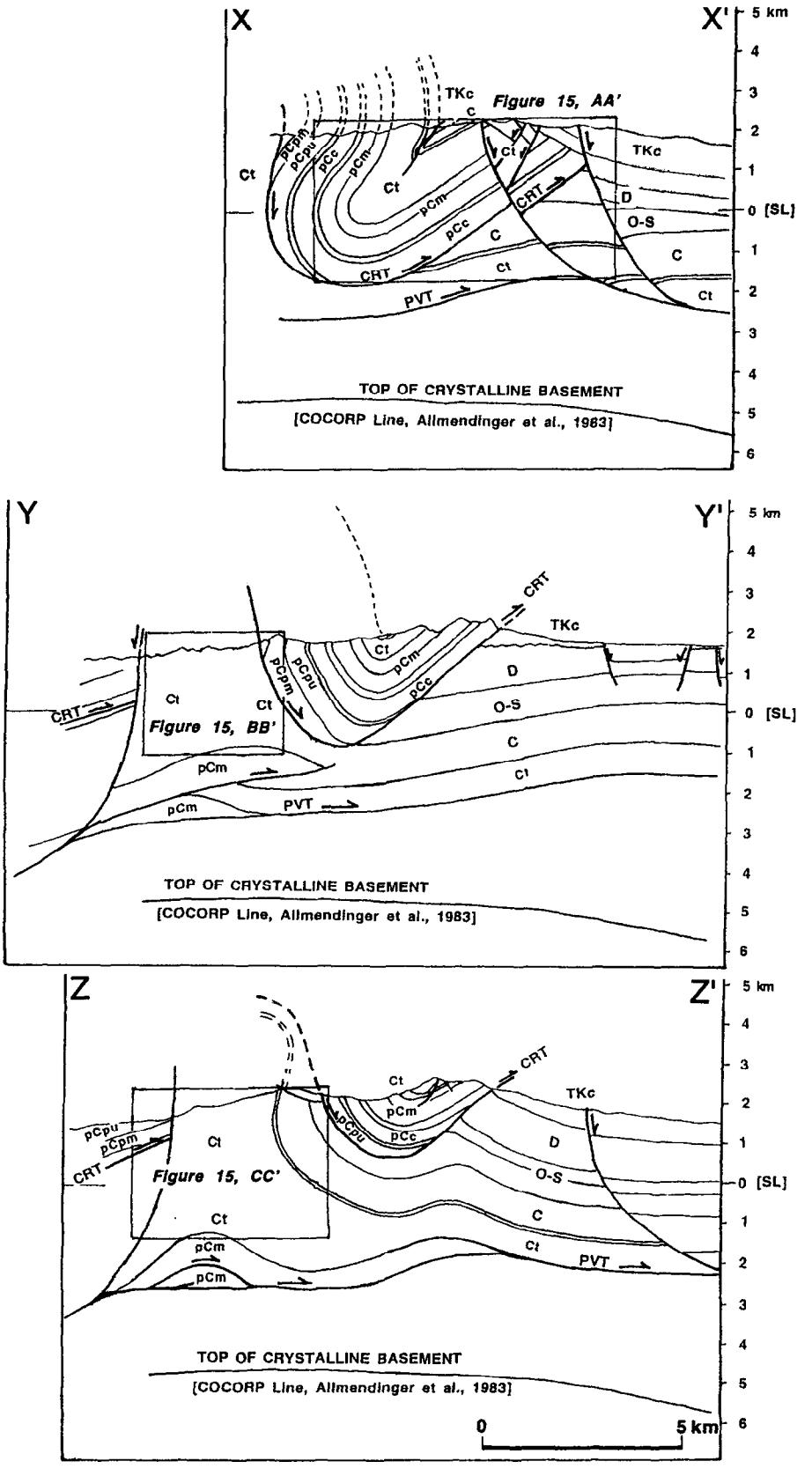

Fig. 14. Cross-sections through the Canyon Range showing the change in geometry of the syncline from an open fold in the south (ZZ') to a tight overturned fold in the north (XX'). Locations of detailed cross-sections (Fig. 15) are shown.

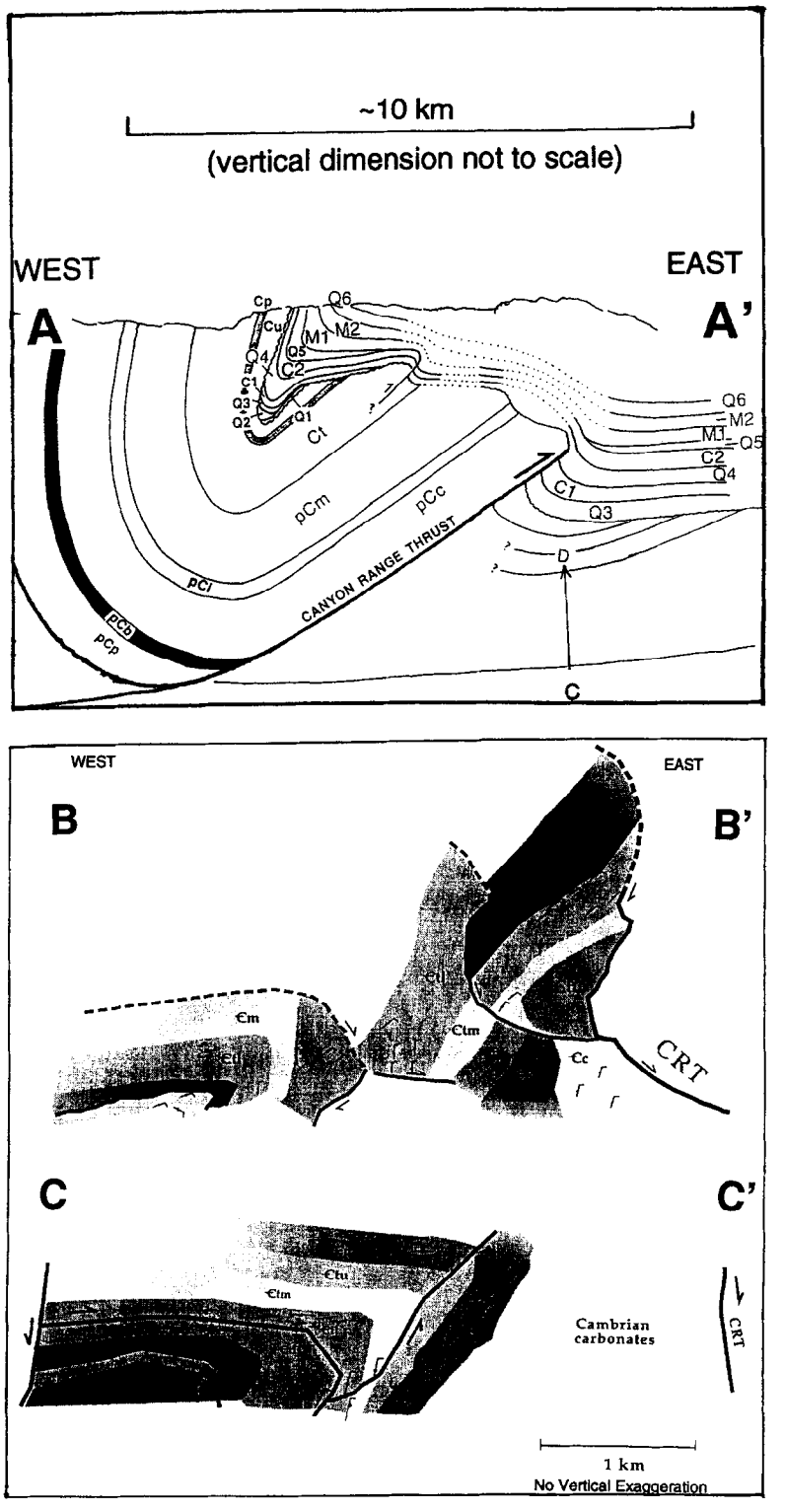

Fig. 15. Schematic composite cross-section (AA′) through the Canyon Range syncline along cross-section line XX′, showing the detailed relationships between the folded Canyon Range thrust and the Canyon Range conglomerates. Clast compositions in the conglomerates are used to define quartzite petrofacies (*Q1*, *Q2*, ...*Q6*), carbonate petrofacies (*C1*, *C2*), and mixed petrofacies (*M1*, *M2*) (DeCelles, personal communication). Details of structures in the anticlinal core on cross-sections YY′ and ZZ′ are shown in down-plunge projections through the antiformal stack in the Canyon Range footwall exposed on the west side of the range. The projection axis in the northern part (BB′) is 7, 184, and that in the southern part (CC′) is 12, 192.

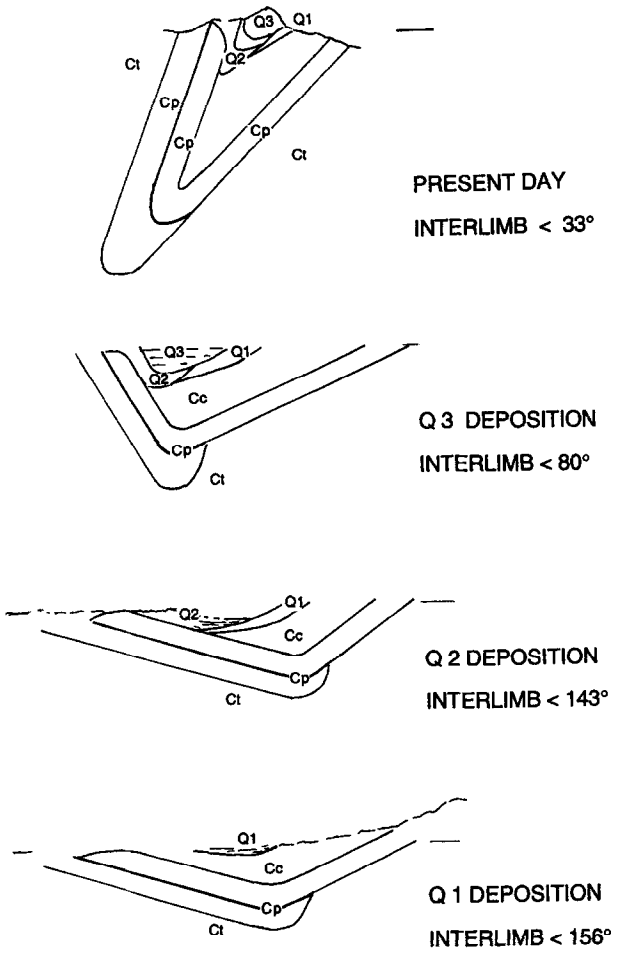

Fig. 16. Unfolding of the Canyon Range syncline in the Dry Creek–Mine Hollow area using successive angular unconformities developed in synorogenic conglomerates in both limbs of the syncline.

steep E–W trending motion plane (Pequera, 1991; Pequera *et al.*, 1994).

Some of the oldest synorogenic conglomerates that are infolded in the syncline are overridden by the thrust along the eastern flank of the range. This allows temporal correlations to be made between conglomerate deposition, fold tightening and thrust reactivation. For example, at the time of conglomerate *Q3* deposition, the fold interlimb angle was 80°, compared to a present-day angle of 33°; thus the fold was tightened by 47° after *Q3* deposition, with ~35° of this tightening achieved by rotation of the western limb. At the same time the thrust was reactivated and overrode *Q3*, with a total additional slip of ~1 km during reactivation. Both fold tightening and thrust motion had stopped by the time of deposition of the uppermost mapped conglomerate unit *Q6* which is undeformed. The thrust reactivation could be interpreted either as the result of additional slip being fed into the thrust from younger, lower faults, or as a result of flexural slip during fold tightening. There is little or no evidence for late-stage flexural slip in the eastern limb of the fold. In addition, the maximum possible flexural slip that could have taken place along a single surface (i.e. the fault plane) for the limb rotation involved after *Q3* deposition is ~0.65 km (using Ramsay, 1967) which does not account for all the reactivation slip that is observed. This suggests that most of the thrust-reactivation slip was transferred to the roof thrust from lower faults.

Fold tightening of the syncline by steepening of its west limb is closely related to growth of the adjoining antiformal structure exposed along the western flank of the range (Fig. 14). The amplification and tightening of the antiform is a direct result of the growth of the antiformal stack in the foot wall of the Canyon Range thrust as a result of imbricates being emplaced off the Pavant thrust. Fold tightening did not start until after the first Canyon Range conglomerates were deposited in Upper Cenomanian times (~93 Ma). Regional timing information reveals that this was well after main movement on the Canyon Range thrust (Upper Neocomian, 130–120 Ma) and the Pavant thrust (Aptian–Albian, 120–100 Ma). Thus both the roof thrust and the floor thrust existed before the imbricates in the antiformal stack were emplaced, and the structure grew as a CSD. As each imbricate was emplaced, a small amount of slip was transferred to the roof thrust (i.e. the Canyon Range thrust), thereby reactivating it and causing it to override its own synorogenic conglomerates.

Microstructural data. In addition to working out timing relationships based on the synorogenic deposits, detailed studies on microstructures developed in quartzites within the antiformal stack allow us to work out the emplacement conditions for the individual horses within the stack (Sussman, 1995). The quartzites from all the horses show microstructures indicating an early phase of high temperature deformation, related to initial emplacement of the Pavant thrust sheet. These microstructures are overprinted by younger features developed during the growth of the antifromal stack. The emplacement of each horse in the stack gives rise to a suite of microstructures in the rocks that reflect the conditions of deformation (Knipe, 1989; Sussman, 1995; Sussman and Mitra, 1995a,b). The microstructures developed within each horse have been quantified on the basis of 500-grain point counts of all microstructural features observed in each sample (Sussman, 1995; Sussman and Mitra, 1995a,b, in review). Comparison of data from different horses (based on 7 to 15 samples from each horse) indicates a distinct trend of increase in cataclasis and decrease in plasticity in going from the higher to the lower horses within the antiformal stack (Sussman, 1995; Sussman and Mitra, 1995a,b, in review).

The microstructural data are important because they indicate that each horse of the duplex was emplaced under different deformation conditions, and indicate that there was a greater amount of overburden on the structure when the first horse was emplaced as compared to later horses. This suggests that the structure was being progressively unroofed as it grew. We use the micro-

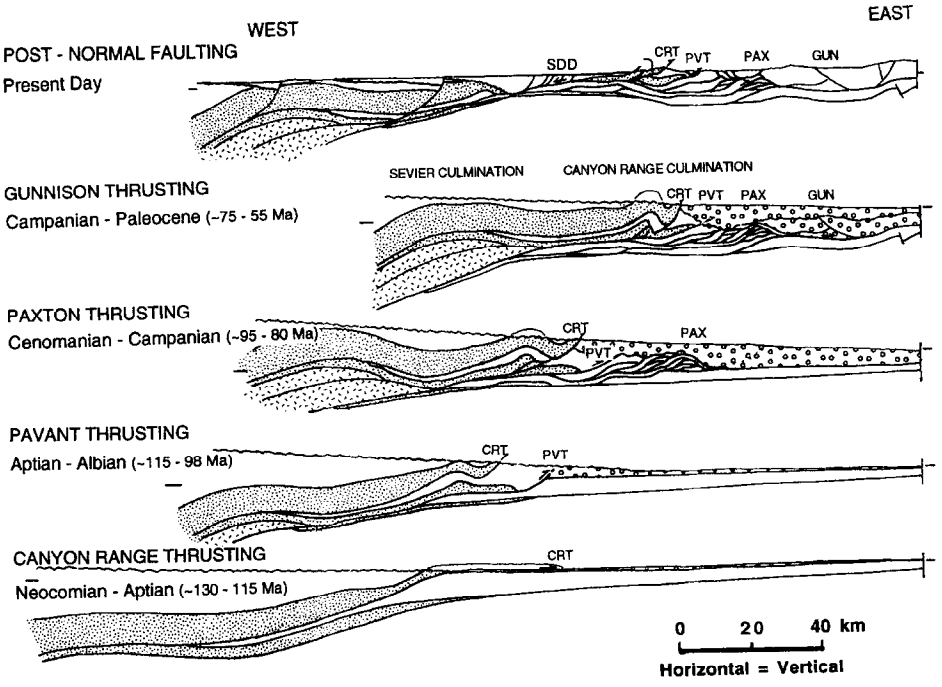

Fig. 17. Kinematic history of the central Utah segment of the Sevier FTB based on an incrementally restored regional balanced cross-section showing the approximate shapes of the orogenic wedge at the time of emplacement of successive major thrusts (based on Coogan *et al.*, 1995). Thrusts shown are Canyon Range (CRT), Pavant (PVT), Paxton (PAX) and Gunnison (GUN); also shown is the Sevier Desert Detachment (SDD), a low-angle normal fault. Granite pattern indicates Precambrian basement rocks, stippled pattern indicates Proterozoic quartzites, and open circle pattern indicates synorogenic sediments.

structural data, in conjunction with timing information from synorogenic deposits and the geometric model for growth of a fault propagation fold connecting splay duplex, to present a kinematic model for the evolution of the Canyon Range structure.

Kinematic history. The kinematic evolution of structures observed in the Canyon Range can be interpreted in the context of regional relations based on step-wise restorations (Fig. 17) of the balanced cross-section shown in Fig. 12. After initial emplacement of the Canyon Range thrust sheet the sheet was eroded down to the level of the Upper Paleozoic section. The sheet was then folded over a ramp in the Pavant thrust at the time of Pavant emplacement forming a broad syncline (Fig. 16) in front of the ramp anticline; erosion continued down to the level of the Proterozoic–Cambrian quartzites before some conglomerates (*Q1*) were preserved in the core of the broad syncline. Deposition of *Q2* is localized to the core of the syncline.

Growth of the first connecting splay off the Pavant thrust formed a fault propagation fold and produced a significant change in the fold geometry of the first order syncline, reducing the interlimb angle to $<80°$ (Fig. 16). Conglomerate *Q3* was deposited at this stage; with erosion through the crest of the structure, Paleozoic carbonate clasts were derived from the back-limb of the anticline forming conglomerate *C1*. When the first connecting splay eventually reached the Canyon Range (roof) thrust it reactivated the thrust causing it to overide *Q3* and *C1* conglomerates at its toe (Fig. 15, AA′). A similar sequence was followed during the growth and eventual breakthrough of the second connecting splay; the forelimb of the anticline was overturned and stretched vertically, conglomerates *Q4* and *C2* were deposited, and the thrust was reactivated forming a fault propagation fold in *Q4* and *C2* (Fig. 15, AA′). The succeeding connecting splays are smaller and do not cause major changes in the structural geometry. Erosional breaching of the duplex culmination led to more sediments being derived from Paleozoic rocks uplifted by the Sevier culmination, giving rise to conglomerates with mixed clast lithologies (*M1* and *M2*).

On the basis of regional and local timing information, structural geometry, and microstructural data we have presented a kinematic model for evolution of structures in the Canyon Range. The growth of the Canyon Range connecting splay duplex allows deformation and thickening to continue in the Canyon Range culmination throughout the time that thrusting is active in this part of the Sevier FTB (Fig. 17). It is clearly a mechanism for maintaining the surface slope necessary for the wedge to remain critical, and counters the effect of surface erosion that tends to reduce taper to a subcritical state. The larger scale driving mechanism that produces the Canyon Range structure, however, lies farther back in the orogenic belt.

The orogenic wedge is made up of two juxtaposed wedges: a rear wedge with high initial taper comprised of stronger rocks, and a frontal wedge with low initial taper

made up of weaker sedimentary rocks (DeCelles and Mitra, 1995). During the late stages of deformation when thrusting progresses into the frontal wedge, taper in the rear wedge is maintained by growth of the Sevier culmination (Fig. 17) with the emplacement of slices of Precambrian crystalline basement in the core of that structure (DeCelles *et al.*, 1995; Mitra, in press). The rheological behavior of the basement and the overlying Proterozoic–Cambrian quartzites are similar under the ambient deformation conditions in this part of the rear wedge (Mitra, in press), so that the quartzites can be pushed up the basal slope and the slip can be transferred directly to the 'toe' of the rear wedge (the miogeocline/shelf hinge). Secondary thickening occurs at the miogeocline/shelf transition zone by growth of a duplex formed by connecting splays between pre-existing thrusts (i.e. the Canyon Range culmination). This thickening creates sufficient structural elevation in the back of the low taper sedimentary wedge for it to become critical, so that thrusting can progress on to the foreland with slip being ultimately transmitted to the frontal Paxton and Gunnison thrusts.

DISCUSSION

There is growing evidence that internal thrust sheets continue to shorten and thicken and are progressively uplifted in the internal portions of a FTB concurrent with the advance of the external FTB on to the foreland. Generally, internal thrust sheets are thicker, have steeper taper, and are made up of stronger rocks (such as crystalline basement or quartzites) than the external FTB sedimentary prism; the strong rear wedge drives the weaker sedimentary wedge in front of it (DeCelles and Mitra, 1995). The actual mechanism by which taper is maintained in the rear wedge may vary depending on a variety of factors, such as lithotectonic stratigraphy of the sedimentary package, original sedimentary taper and how it varies from the miogeocline to the shelf, deformation conditions and rheologic behavior of the rocks involved in the deformation (Mitra, in press).

Continued duplexing in the rear wedge is one way of thickening the section there and maintaining taper; because of the significantly larger scale of structures developed in the rear wedge (Boyer and Mitra, 1988) this helps to maintain taper in the FTB wedge as a whole. We have shown, with the help of previously documented examples, that continued basement duplexing or reactivation of pre-existing horses in an internal duplex are two possible mechanisms for thickening the rear wedge to maintain taper. We have also described (with a well-constrained example) a new mechanism of late-stage duplexing (*connecting splay duplexing*) that may be equally important in thickening the rear wedge and maintaining taper in the FTB wedge as a whole. Because of their geometric similarity to typical duplexes (Boyer and Elliott, 1982) CSDs may have been previously unrecognized; our study suggests that they may play an important role in the kinematic evolution of FTBs.

Acknowledgements—This work benefited from discussions with many colleagues, particularly the structural geology group at the University of Rochester, and Peter DeCelles and Jim Coogan. Thoughtful reviews by Ron Bruhn and Dave Wiltschko, and the guest editor Don Fisher were also very helpful. Acknowledgement is made to the donors of the Petroleum Research Fund, administered by the American Chemical Society, for partial support of this research through grant 21954-AC2; field work by AJS was also partly supported by a Penrose Research Grant from the Geological Society of America, a Sigma Xi Research Grant and the Pequera Memorial Scholarship from the University of Rochester.

REFERENCES

Allmendinger, R. W. (1992) Fold and thrust tectonics of the western United States exclusive of the accreted terranes. In *The Cordilleran Orogen, the Conterminous U.S.*, eds B. C. Burchfiel, P. W. Lipman and M. L. Zoback, Geological Society of America, The Geology of North America **G-3**. 583–608.

Allmendinger, R. W., Sharp, J. W., Von Tish, D., Serpa, L., Brown, L., Oliver, J., Kaufman, S. and Smith, R. B. (1983) Cenozoic and Mesozoic structure of the eastern Basin and Range province, Utah, from COCORP seismic reflection data. *Geology* **11**, 532–536.

Armstrong, R. L. (1968) Sevier orogenic belt in Nevada and Utah. *Bulletin of the Geological Society, America* **79**, 429–458.

Armstrong, F. C. and Oriel, S. S. (1965) Tectonic development of the Idaho–Wyoming thrust belt. *Bulletin of the American Association of Petroleum Geologists* **49**, 1847–1866.

Boyer, S. E. (1992a). Sequential development of the southern Blue Ridge province of northwest North Carolina ascertained from the relationships between penetrative deformation and thrusting. In *Structural Geology of Fold and Thrust Belts*, eds S. Mitra and G. W. Fisher, pp. 161–188. Johns Hopkins Univ. Press, Baltimore.

Boyer, S. E. (1992b). Geometric evidence for synchronous thrusting in the southern Alberta and northwest Montana thrust belts. In *Thrust Tectonics*, ed. K. R. McClay, pp. 377–390. Chapman and Hall, London.

Boyer, S. E. (1995) Sedimentary basin taper as a factor controlling the geometry and advance of thrust belts. *American Journal of Science* **295**, 1220–1254.

Boyer, S. E. and Elliott, D. (1982) Thrust systems. *Bulletin of the American Association of Petroleum Geologists* **66**, 1196–1230.

Boyer, S. E. and Mitra, G. (1988) Deformation of the basement-cover transition zone of the Appalachian Blue Ridge Province. In *Geometry and Mechanisms of Thrusting, with Special Reference to the Appalachians*, eds G. Mitra and S. Wojtal, Geological Society of America Special Paper **222**, 119–136.

Bruhn, R. L. and Beck, S. L. (1981) Mechanics of thrust faulting in crystalline basement, Sevier orogenic belt, Utah. *Geology* **9**, 200–204.

Burchfiel, B. C. and Davis, G. A. (1975) Nature and controls of Cordilleran orogenesis, western United States — extensions of an earlier synthesis. *American Journal of Science* **275A**, 363–396.

Burchfiel, B. C. and Hickcox, C. W. (1972) Structural development of central Utah. In *Plateau–Basin and Range Transition Zone, Central Utah*, eds J. L. Baer and E. Callaghan, 2, 55–66. Utah Geological Association Publication.

Chapple, W. M. (1978) Mechanics of thin-skinned fold-and-thrust belts. *Bulletin of the Geological Society, America* **89**, 1189–1198.

Christiansen, R. F. (1952) Structure and stratigraphy of the Canyon Range, Utah. *Bulletin of the Geological Society of America* **63**, 717–740.

Coogan, J. C., DeCelles, P. G., Mitra, G. and Sussman, A. J. (1995) New regional balanced cross-section across the Sevier desert region and the Central Utah thrust belt. *Geological Society of America Rocky Mountain Meeting Abstracts* **27**, 7.

Coward, M. P. and Butler, R. W. H. (1985) Thrust Tectonics and Deep Structure of the Pakistan Himalayas. *Geology*, **13**, 417–420.

Currie, B. S. (in press) Upper Jurassic–Lower Cretaceous Morrison and Cedar Mountain Formations, NE Utah–NW Colorado: Relationships between nonmarine deposition and early Cordilleran foreland basin development. In *The Upper Jurassic Morrison Formation: An*

Interdisciplinary Evaluation, eds by K. Carpenter *et al.* Geological Society of America Special Paper.

Dahlen, F. A. (1990) Critical taper model of fold-and-thrust belts and accretionary wedges. *Annual Reviews of Earth and Planetary Science* **18**, 55–99.

Davis, D., Suppe, J. and Dahlen, F. A. (1983) Mechanics of fold-and-thrust belts and accretionary wedges. *Journal of Geophysical Research* **88**, 1153–1172.

DeCelles, P. G. (1994) Late Cretaceous–Paleocene synorogenic sedimentation and kinematic history of the Sevier thrust belt, northeast Utah and southwest Wyoming. *Bulletin of the Geological Society of America* **106**, 32–56.

DeCelles, P. G. and Mitra, G. (1995) History of the Sevier orogenic wedge in terms of critical taper models, northeast Utah and southwest Wyoming. *Bulletin of the Geological Society of America* **107**, 454–462.

DeCelles, P. G., Gray, M. B., Ridgway, K. D., Cole, R. B., Srivastava, P., Pequera, N. and Pivnik, D. A. (1991) Kinematic history of a foreland uplift from Paleocene synorogenic conglomerate, Beartooth Range, Wyoming and Montana. *Bulletin of the Geological Society of America* **103**, 1458–1475.

DeCelles, P. G., Lawton, T. F. and Mitra, G. (1995) Timing of Sevier thrusting, central Utah. *Geology* **23**, 699–702.

Elliott, D. and Johnson, M. R. W. (1980) Structural evolution in the northern part of the Moine thrust belt, NW Scotland. *Transactions of the Royal Society of Edinburgh, Earth Sciences* **71**, 69–96.

Gilluly, J. (1960) A folded thrust in Nevada — inferences as to time relations between fold and faulting. *American Journal of Science* **258A**, 68–79.

Harris, L. D. (1978) Similarities between the thick-skinned Blue Ridge anticlinorium and the thin-skinned Powell Valley anticline. *Bulletin of the Geological Society of America Part I* **90**, 525–539.

Higgins, J. M. (1982) Geology of the Champlin Peak quadrangle, Juab and Millard counties, Utah. *Brigham Young University Geology Studies* **29**, 40–58.

Hintze, L. F. (1980) Geologic map of Utah. Utah Geological and Mineral Survey, scale 1:500,000.

Holladay, J. C. (1983) Geology of the northern Canyon Range, Millard and Juab counties, Utah. *Brigham Young University Geology Studies* **31**, 1–28.

Jordan, T. E. (1981) Thrust loads and foreland basin development, Cretaceous, western United States. *Bulletin of the American Association of Petroleum Geologists* **65**, 2506–2520.

Knipe, R. J. (1989) Deformation mechanisms — recognition from natural tectonites. *Journal of Structural Geology* **11**, 127–146.

Lamerson, R. (1982) *The Fossil Basin and its Relationship to the Absaroka Thrust System, Wyoming and Utah*, pp. 279–340. *Rocky Mountain Association of Geology Symposium.*

Lawton. T. F. (1982) Lithofacies correlations within the Upper Cretaceous Indianola Group. In *Overthrust Belt of Utah*, ed D. L. Nielson, Utah Geological Association Publication. 10, 199–213.

Lawton, T. (1985) Style and timing of the frontal structures, Sevier thrust belt, central Utah. *Bulletin of the American Association of Petroleum Geology* **69**, 1145–1159.

Mandl, G. (1988) *Mechanics of Tectonic Faulting: Models and Basic Concepts.* Elsevier Publishing Co., Amsterdam.

Millard, A. W. Jr (1983) Geology of the southwestern quarter of the Scipio North (15-minute) quadrangle, Millard and Juab counties, Utah. *Brigham Young University Geologists Studies* **30**, 59–81.

Miller, D. M., Nilsen, T. H. and Bilodeau, W. L. (1992) Late Cretaceous to early Eocene geologic evolution of the U.S. Cordillera. In *The Cordilleran Orogen, the Conterminous U.S.*, eds B. C. Burchfiel, P. W. Lipman and M. L. Zoback, Geological Society of America, The Geology of North America **G-3**. 205–260.

Mitra, G. (1979) Ductile deformation zones in Blue Ridge basement rocks and estimation of finite strains. *Bulletin of the Geological Society of America Part I* **90**, 935–951.

Mitra, S. (1978) Microscopic deformation mechanisms and flow laws in quartzites within the South Mountain anticline. *Journal of Geology* **86**, 129–152.

Mitra, S. (1986) Duplex structures and imbricate thrust systems: Geometry, structural position and hydrocarbon potential. *Bulletin of the American Association of Petroleum Geologists* **70**, 1087–1112.

Mitra, G. (1994) Strain variation in thrust sheets across the Sevier fold-and-thrust belt (Idaho–Utah–Wyoming): implications for section restoration and wedge taper evolution. *Journal of Structural Geologists* **16**, 585–602.

Mitra, G. (in press) Evolution of Salients in a Fold-and-Thrust Belt: the Effects of Sedimentary Basin Geometry, Strain Distribution and Critical Taper. In *Evolution of Geologic Structures from Macro- to Micro-Scales*, ed. S. Sengupta. Chapman and Hall, London.

Mitra, G. and Elliott, D. (1980) Deformation of basement in the Blue Ridge and the development of the South Mountain cleavage. Proceedings Caledonides in the USA: I.G.C.P. Project 27. Caledonide Orogen. *Va. Polytech. Institute and State University Memoir* **2**, 307–312.

Mitra, G. and Boyer, S. E. (1986) Energy balance and deformation mechanisms of duplexes. *Journal of Structural Geology* **8**, 291–304.

Mitra, G., Pequera, N., Sussman, A. J. and DeCelles, P. G. (1994) Evolution of structures in the Canyon Range thrust sheet (Sevier fold-and-thrust belt) based on field relations and microstructural studies. *Geological Society of America Annual Meeting Abstracts* **26**, A527.

Mitra, G., Sussman, A., Pequera, N., DeCelles, P. G. and Coogan, J. (1995) Structural evolution of the Canyon Range, Central Utah Sevier orogenic wedge: implications for critical taper during thrusting. *Geological Society of America, Rocky Mountain Meeting Abstracts* **27**, 47.

Otton, J. K. (1995) Western frontal fault of the Canyon Range: Is it the breakaway zone of the Sevier Desert detachment? *Geology* **23**, 547–550.

Pequera, N. (1991) Growth history of a fault-propagation fold: An example from the Canyon Range, central Utah. M.Sc. thesis, University of Rochester.

Pequera, N., Mitra, G. and Sussman, A. J. (1994) The Canyon Range thrust sheet in the Sevier fold-and-thrust belt of central Utah: deformation history based on structural analysis. *Geological Society of America Rocky Mountain, Section Meeting Abstracts* **26**, 58.

Ramsay, J. G. (1967) *Folding and Fracturing of Rocks.* McGraw-Hill Book Co., New York.

Ramsay, J. G., Casey, M. and Kligfield, R. (1983) Role of shear in development of the Helvetic fold-thrust belt of Switzerland. *Geology* **11**, 439–442.

Ramsay, J. G. and Huber, M. I. (1983) *The Techniques of Modern Structural Geology Volume 1: Strain Analysis.* Academic Press, London.

Rodgers, J. (1995) Lines of basement uplifts within the external parts of orogenic belts. *American Journal of Science* **295**, 455–487.

Roeder, D. South-Alpine thrusting and trans-Alpine convergence. In *Alpine Tectonics*, eds M. P. Coward, D. Dietrich and R. G. Park, Geological Society Special Publication. 45, 211–227.

Roeder, D., Gilbert, E. and Witherspoon, W. (1978) *Evolution and Macroscopic Structure of Valley and Ridge Thrust Belt, Tennessee and Virginia.* University of Tennessee, Studies in Geology **2**.

Royse, F. (1993) Case of the phantom foredeep: Early Cretaceous in west-central Utah. *Geology* **21**, 133–136.

Royse, F., Warner, M. A. and Reese, D. L. (1975) *Thrust belt Strucural Geometry and Related Stratigraphic Problems, Wyoming–Idaho–northern Utah.* Rocky Mountain Association Geology Symposium. 41–45.

Schirmer, T. W. (1988) Structural analysis using thrust-fault hanging-wall sequence diagrams: Ogden duplex, Wasatch Range, Utah. *Bulletin of the American Association of Petroleum Geologists* **72**, 573–585.

Schonborn, G. (1992) Alpine tectonics and kinematic models of the central Southern Alps. *Memorie di Scienze Geologiche Institut di Geologia e Mineralogia dell'Università di Padova* **44**, 229–393.

Schwans, P. (1988) Depositional response of Pigeon Creek Formation, Utah, to initial fold-thrust belt deformation in a differentially subsiding foreland basin. In *Interaction of the Rocky Mountain Foreland and Cordilleran Thrust Belt*, eds C. J. Schmidt and W. J. Perry, Geological Society of America Memoir. 171, 531–556.

Schwartz, R. K. and DeCelles, P. G. (1988) Cordilleran foreland-basin evolution and synorogenic sedimentation in response to interactive Cretaceous thrusting and reactivated foreland partitioning. In *Interaction of the Rocky Mountain Foreland and Cordilleran Thrust Belt*, eds C. J. Schmidt and W. J. Perry, Geological Society of America Memoir. 171, 489–514.

Sprinkel, D. A., Weiss, M. P. and Fleming, R. W. (1992) Stratigraphic reinterpretation of a synorogenic unit of Early Cretaceous age, Sevier orogenic belt, central Utah. *Geological Society of America Rocky Mountain Section Abstracts* **24**, 63.

Standlee, L. A. (1982) Structure and stratigraphy of Jurassic rocks in central Utah: Their influence on tectonic development of the Cordil-

leran foreland thrust belt. In *Geologic Studies of the Cordilleran foreland thrust belt*, ed. R. B. Powers, pp. 357–382. Rocky Mountain Association of Geologists.

Stanley, R. and Ratcliffe, N. (1983) *Simplified Lithotectonic Synthesis of Pre-Silurian Rocks in Western New England.* Vermont Geol. Survey Special Bulletin 5.

Sussman, A. J. (1995) Geometry, deformation history and kinematics in the footwall of the Canyon Range thrust, central Utah. M.Sc. thesis, Universtiy of Rochester.

Sussman, A. J. and Mitra, G. (1995) Deformation patterns in the footwall of the Canyon Range thrust, central Utah: implications for Sevier fold-and-thrust belt development. *Geological Society of America, Rocky Mountain Meeting Abstracts* **27**, 57.

Sussman, A. J. and Mitra, G. (1995) Structural evolution of a connecting splay duplex: an example based on field and microstructural studies in the footwall of the Canyon Range thrust, Utah. *Geological Society of America Annual Meeting Abstracts* **27**, A122.

Talling, J., Burbank, D. W., Hobbs, R. S., Lawton, T. L. and Lund, S. P. (1994) Magnetostratigraphic chronology of Cretaceous to Eocene thrust belt evolution, central Utah. *Journal of Geology* **102**, 181–196.

Villien, A. and Kligfield, R. M. (1986) Thrusting and synorogenic sedimentation in central Utah. In *Paleotectonics and Sedimentation in the Rocky Mountain Region, United States*, ed. J. A. Peterson, American Association of Petroleum Geologists Memoirs. 41, 281–308.

Wiltschko, D. V. and Dorr, J. A. (1983) Timing of deformation in overthrust belt and foreland of Idaho, Wyoming and Utah. *Bulletin of the American Association of Petroleum Geologists* **67**, 1304–1322.

Woodward, N. B., editor, (1985) *Valley and Ridge Thrust Belt: Balanced Structural Sections, Pennsylvania to Alabama.* University of Tennesse, Studies in Geology 12.

Woodward, N. B. (1987) Geological applicability of critical wedge theory. *Bulletin of the Geological Society of America* **99**, 827–832.

Woodward, N. B., Gray, D. R. and Spears, D. B. (1986) Including strain data in balanced cross-sections. *Journal of Structural Geology* **8**, 313–324.

Woodward, N. B., Boyer, S. E. and Suppe, J. (1989) *Balanced Geological Cross-sections: An Essential Technique in Geologic Research and Exploration.* 28th International Geological Congress, Short Course in Geology 6, American Geophysics Union.

Yingling, V. and Heller, P. L. (1992) Timing and record of foreland sedimentation during initiation of the Sevier orogenic belt in central Utah. *Basin Research* **4**, 279–290.

Yonkee, W. A. (1992) Basement-cover relations, Sevier orogenic belt, northern Utah. *Bulletin of the Geological Society of America* **104**, 280–322.

Yonkee, W. A. and Mitra, G. (1993) Comparision of basement deformation styles in the Rocky Mountain Foreland and Sevier Orogenic Belt. In *Basement Behavior in Rocky Mountain Foreland Structure*, eds C. Schmidt, R. Chase, and E. Erslev, Geological Society of America Special Paper. 280, 197–228.